有机化学 DOI: 10.6023/cjoc202302019 研究论文
Chinese Journal of Organic Chemistry ARTICLE

金属-有机框架衍生的植酸铁催化氢转移高效制备 2-芳基苯并噁唑

欧世国 柴瑞瑞 李家豪 王大伟* 桑欣欣*
(江南大学化学与材料工程学院 教育部合成与生物胶体重点实验室 江苏无锡 214122)

摘要 金属有机框架及其衍生物在催化领域显示出巨大的应用潜力. 利用表面工程方法制备了 ZIF-L-Co@phytate-iron (ZIF-L-Co@PA-Fe)异质金属-有机框架(MOF)衍生物. 首先, 通过植酸(PA)与 ZIF-L-Co 框架中的有机配体交换, 制备植酸功能化的 ZIF-L-Co@PA 材料. 然后, 通过 Fe^{3+}与配体的配位合成了具有独特异质结构的 ZIF-L-Co@PA-Fe. 得益于金属-配体相互作用的改进, 所设计的 ZIF-L-Co@PA-Fe 杂化物对氢转移反应表现出优异的催化活性. 以 ZIF-L-Co@PA-Fe 为催化剂, 在无溶剂条件下成功地实现了邻硝基苯酚与醇的转移氢环化反应, 得到2-取代苯并噁唑衍生物. 该催化反应不需要氧化剂、还原剂或碱等额外的添加剂. 此外, ZIF-L-Co@PA-Fe 配合物具有良好的催化循环稳定性, 可重复使用 5 次而催化活性无明显下降. 本工作可为优化其他系列 MOF 衍生物的催化性能提供有效的指导.
关键词 金属-有机框架; 离子交换; 多相催化; 氢转移

Metal-Organic Framework Derived Phytate-Iron for Efficient Synthesis of 2-Arylbenzoxazole via Hydrogen Transfer Strategy

Ou, Shiguo Chai, Ruirui Li, Jiahao Wang, Dawei* Sang, Xinxin*
(*Key Laboratory of Synthetic and Biological Colloids*, *Ministry of Education*, *School of Chemical and Material Engineering*, *Jiangnan University*, *Wuxi*, *Jiangsu 214122*)

Abstract Recently, metal-organic framework (MOF) and its derivatives showed great application potential in catalysis. ZIF-L-Co@phytate-iron (ZIF-L-Co@PA-Fe) heterogeneous MOF derivatives were synthesized by a facile surface engineering method. Phytic acid functionalized ZIF-L-Co (ZIF-L-Co@PA) was firstly prepared through organic ligand exchange of phytic acid (PA). Then, ZIF-L-Co@PA-Fe with unique heterostructure was prepared via coordination occurred between Fe^{3+} and ligands. Benefiting from the greatly modify metal-ligand interactions, the as-designed ZIF-L-Co@PA-Fe hybrids exhibited excellent catalytic activities toward the hydrogen transfer reactions. 2-Substituted benzoxazole derivatives were successfully synthesized via transfer hydrogenative annulation of *o*-nitrophenol with alcohols catalyzed by ZIF-L-Co@PA-Fe under solvent-free conditions. No additional additives, such as oxidants, reductants or bases were required for this reaction. Moreover, ZIF-L-Co@PA-Fe coordination complex showed excellent reusability and could be recycled up to five times without obvious decline in its catalytic activity. This work may provide effective guidance for optimizing the catalytic performance of other series of MOF derivatives.
Keywords metal-organic framework; ion exchange; heterogeneous catalysis; hydrogen transfer

1 Introduction

Benzoxazoles as a kind of five-membered N-containing heterocycles are important building blocks for pharmaceuticals, agrochemical compounds, bioactive molecules and functional materials.[1] The synthesis of benzoxazole and its derivatives has attracted much attention. Typically, benzoxazoles can be synthesized via transition metal-catalyzed intramolecular cyclization reaction from *o*-haloanilides or their analogues.[2] Yet, such synthetic protocols often require toxic oxidants and exhibit low functional group tolerance. Another synthetic pathway for benzoxazoles involves condensation of 2-aminophenols with aldehydes.[3] However, the instability of aldehydes restricts the flexibility of the reactions. Hydrogen transfer provides a powerful and sustainable method for the synthesis of benzoazoles without any external reducing agents.[4] Therefore, readily available and stable alcohols as low-oxidation-level feedstock are good candidates for benzoxazoles formation via a hydroge transfer methodol-

* Corresponding authors. E-mail: sangxx@jiangnan.edu.cn; wangdw@jiangnan.edu.cn
Received February 16, 2023; revised March 19, 2023; published online April 7, 2023.
Project supported by the National Natural Science Foundation of China (No. 21803025).
国家自然科学基金(No. 21803025)资助项目.

 © 2023 Shanghai Institute of Organic Chemistry, Chinese Academy of Sciences

ogy.

Generally, *o*-aminophenol is supplied as the starting materials for the preparation of 2-arylbenzoxazoles with alcohols.[5] Using borrowing hydrogen methodology, alcohols and nitroarenes can directly construct C—N bond.[6] *In situ* reduction of nitrobenzene to aniline was achieved using hydrogen borrowed from the oxidation step of alcohol. This approach provides a one-pot reaction for benzoxazole formation using nitroarenes and alcohols without any external reducing reagents and oxidizers. In 2012, Deng *et al.*[7] developed an iron-catalyst one-pot method for the efficient synthesis of benzoxazoles from 2-nitrophenol and benzyl alcohols. Hong group[8] expanded the synthesis of benzoxazoles from nitroaromatics and alcohols by using iron complexes as the catalyst. In 2018, Wang *et al.*[9] reported that heterogeneous catalyst Au/TiO_2 could catalyze the formation of 2-arylbenzoxazole with a yield about 99%. Ghosh *et al.*[10] developed cheap metal catalysts, such as γ-MnO_2 and CuNiFe magnetic nanocatalyst, which could be used for benzoxazole production with good yields. However, main limitations of these procedures consist were the use of toxic reaction media, additional oxidizing reagents and expensive or labile ligands. Therefore, it is important to develop efficient and readily available catalysts for benzoxazole formation under solvent-free and additive-free conditions.

Zeolitic imidazolate frameworks (ZIFs), as a subfamily of metal organic frameworks (MOFs), are assembled from imidazoles and metal clusters with zeolite-type topology.[11] The high porosity, compositional flexibility together with versatile functionalization endow ZIFs promising application in heterogeneous catalysis.[12] However, the catalytic performance of pristine ZIFs is greatly restricted by the high degree of crystallinity, microporous structure and saturated metal sites. Fortunately, the easy modification of ZIFs enriches the origin of more active sites applicable for expanding their catalysis reaction scopes. Post-synthetic modulations of ZIFs, including destruction, installation, and ion exchange, are regarded as versatile methods to systematically tailor ZIF structures.[13] Herein, a two-dimensional (2D) Co-based leaf-like ZIF-L-Co was post-modified by phytic acid and Fe^{3+}. Phytic acid as a sustainable bio-based phosphorus-containing organic acid, has strong chelating ability with various metal ions for complex creation. Ligand exchange of ZIF-L-Co firstly occurred between 2-methylimidazole and phytic acid. Then the phosphate groups in PA show hard Lewis-base nature in the coordination with metal ions, improving the coordination ability of materials with Fe^{3+} ions. Owning to the hybrid composition, structural inheritance of ZIF-L-Co and extensive exposure of the active sites, ZIF-L-Co@PA-Fe hybrids exhibit enhanced catalytic activity and stability towards hydrogen transfer reactions for benzoxazole synthesis.

2 Results and discussion

2.1 Preparation and characterization of ZIF-L-Co@PA-Fe

The catalytic performance of MOFs can be conveniently regulated by introduction of foreign metal ions or ligands into a pristine structure via exchange reactions. ZIF-L, with its unique cushion-like cavities and leaf-like morphology, has attracted much attention in catalysis due to its low diffusive resistance and many exposed active sites.[14] ZIF-L derived hybrid ZIF-L-Co@PA-Fe from both ligand and cation exchange was designed via a surface engineering method. The schematic illustration for ZIF-L-Co@PA-Fe preparation is depicted in Scheme 1. The 2D ZIF-L-Co nanosheets were prepared according to a reported method.[15] PA molecule as multi-dentate ligands was then coated on the surface of ZIF-L-Co via the ligand exchange between 2-methylimidazole and PA, forming ZIF-L-Co@PA leaf-like particles. Based on the soft-hard acid-base theory, the hard Lewis-base nature of PA allows regulation of the driving force for the cation exchange.[16] Co^{2+} ions have a moderate co-ordination strength with PA, and Co^{2+} ions in the frameworks of ZIF-L-Co@PA are possible to be displaced by metal ions with stronger Lewis acidity. Fe^{3+} as a typical hard-acid is introduced to the framework via cation exchange of the parent Co^{2+} ions, resulting in the formation of ZIF-L-Co@PA-Fe metal-organic hybrids.

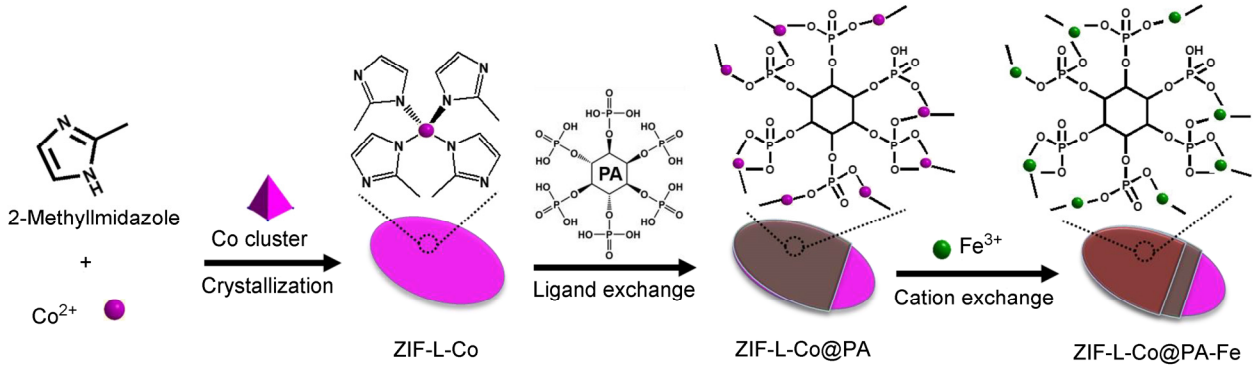

Scheme 1 Schematic illustration of the preparation of ZIF-L-Co@PA-Fe hybrids

 © 2023 Shanghai Institute of Organic Chemistry, Chinese Academy of Sciences

The morphological and compositional characterizations of ZIF-L-Co@PA-Fe were investigated. A leaf-like morphology of ZIF-L-Co could be observed from scanning electron microscope (SEM) image (Figure 1, a), which is similar to that reported in the literature.[15] After etching with phytic acid, ZIF-L-Co@PA still presented a leaf-like morphology (Figure 1, b). The morphology of final ZIF-L-Co@PA-Fe hybrid is depicted in Figure 1c. The leaf-like nanosheets disappeared and irregular crinkly sheet structure could be seen. This observation suggests that Fe^{3+} ions have stronger coordination strength with PA in comparison to Co^{2+} ions. Energy dispersive spectroscopy (DES) study of ZIF-L-Co@PA and ZIF-L-Co@PA-Fe showed obvious composition variation compared with the original ZIF-L-Co. 2-Methylimidazole and Co^{2+} were partially replaced by PA and Fe^{3+}. The crystalline structures before and after exchanges were verified by X-ray diffraction analysis. Although the crystalline structure was destroyed after PA etching, the multi-dentate character of PA facilitates the preservation of the coordination structure and the morphology. This flaky morphology with retained ZIF-L-Co structure may contribute to the improved catalytic activity of ZIF-L-Co@PA-Fe. FT-IR spectra of ZIF-L-Co, ZIF-L-Co@PA and ZIF-L-Co@PA-Fe are revealed in Figure 1d. The out-of-plane and in-plane bending bands of the imidazole ring are observed at 600～800 and 900～1350 cm^{-1}, respectively. The corresponding stretching bands of imidazole are locate between 1350～1500 cm^{-1}. The peak at 1565 cm^{-1} is assigned to the bending vibration of N—H.[17] New peaks appear at 3260, 1635 and 1056 cm^{-1} arised from the phosphoric acid of PA in ZIF-L-Co@PA. Obviously, characteristic peaks of imidazole still exist after ligand exchange. Upon cation exchange, ZIF-L-Co@PA-Fe has a similar spectrum to ZIF-L-Co@PA but with peak intensity reduction of imidazole. Accordingly, exchange reactions successfully occurred and resulted in the formation of ZIF-L-Co@PA-Fe hybrids.

The surface composition and chemistry state of ZIF-L-Co@PA-Fe were further studied by X-ray photoelectron spectroscopy (XPS). The feature peaks of C 1s, N 1s, Co 2p, Fe 2p, O 1s, and P 2p are raised in the XPS survey spectrum (Figure 2). C 1s shown in Figure 2b is deconvoluted into five peaks with binding energies of 283.88, 284.78, 286.28, 286.78, 288.48 eV, which are assigned to C＝C, C—C, C—N, C—O and C＝N bonds, respectively. The appearance of C—N and C＝N bonds is due to partial residual 2-methylimidazole.[18] The N 1s spectrum in Figure 2c is decomposed to three peaks. The peaks at 399.68 and 400.68 eV correspond to the N—C and N—Co/N—Fe, respectively. Furthermore, the peak located at 406.88 eV is assigned to the nitrogen on nitro group.[19] As shown in Figure 2d, the O 1s region is fitted by three disparate peaks, and the peaks at 531.78 eV, 532.38 and 533.28 eV are assigned to O＝P, O—Co/O—Fe and O—C/O—P, respectively.[20] The high-resolution spectrum of Fe 2p is shown in Figure 2f. The peak positions of Fe $2p_{3/2}$ and Fe $2p_{1/2}$ are at 711.78 and 725.38 eV with two broadened satellite peaks simultaneously. The peak at 711.38 eV is split into two peaks, the first one at 711.38 eV for Fe^{2+} while the second one at 712.08 eV for Fe^{3+} species. The peaks centered at 715.28 and 718.68 eV were attributed to satellite peaks.[21]

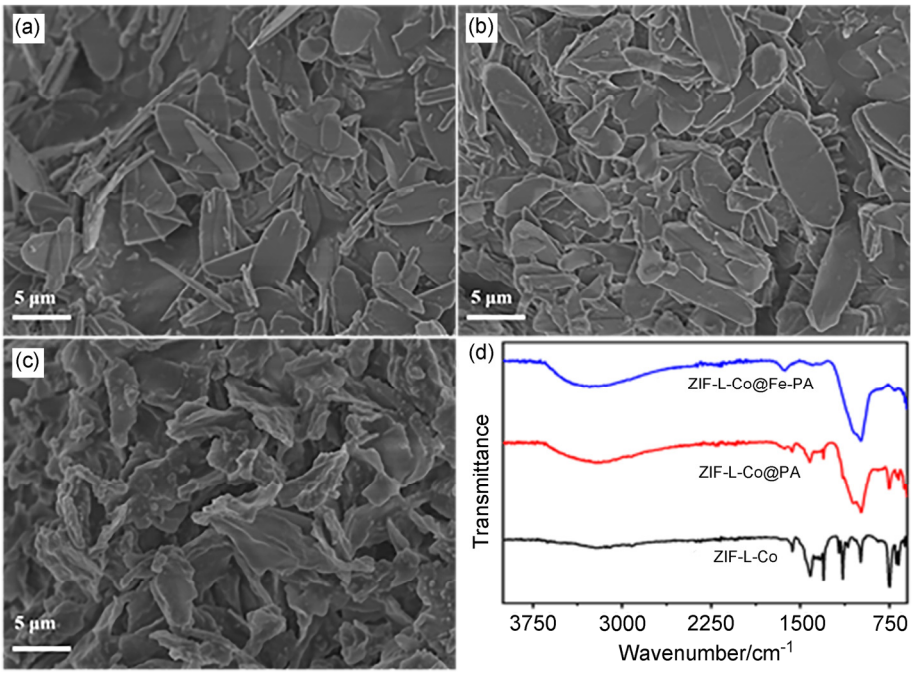

Figure 1 SEM images of (a) ZIF-L-Co, (b) ZIF-L-Co@PA and (c) ZIF-L-Co@PA-Fe, and (d) FT-IR spectra of ZIF-L-Co@PA-Fe, ZIF-L-Co@PA and ZIF-L-Co

 © 2023 Shanghai Institute of Organic Chemistry, Chinese Academy of Sciences

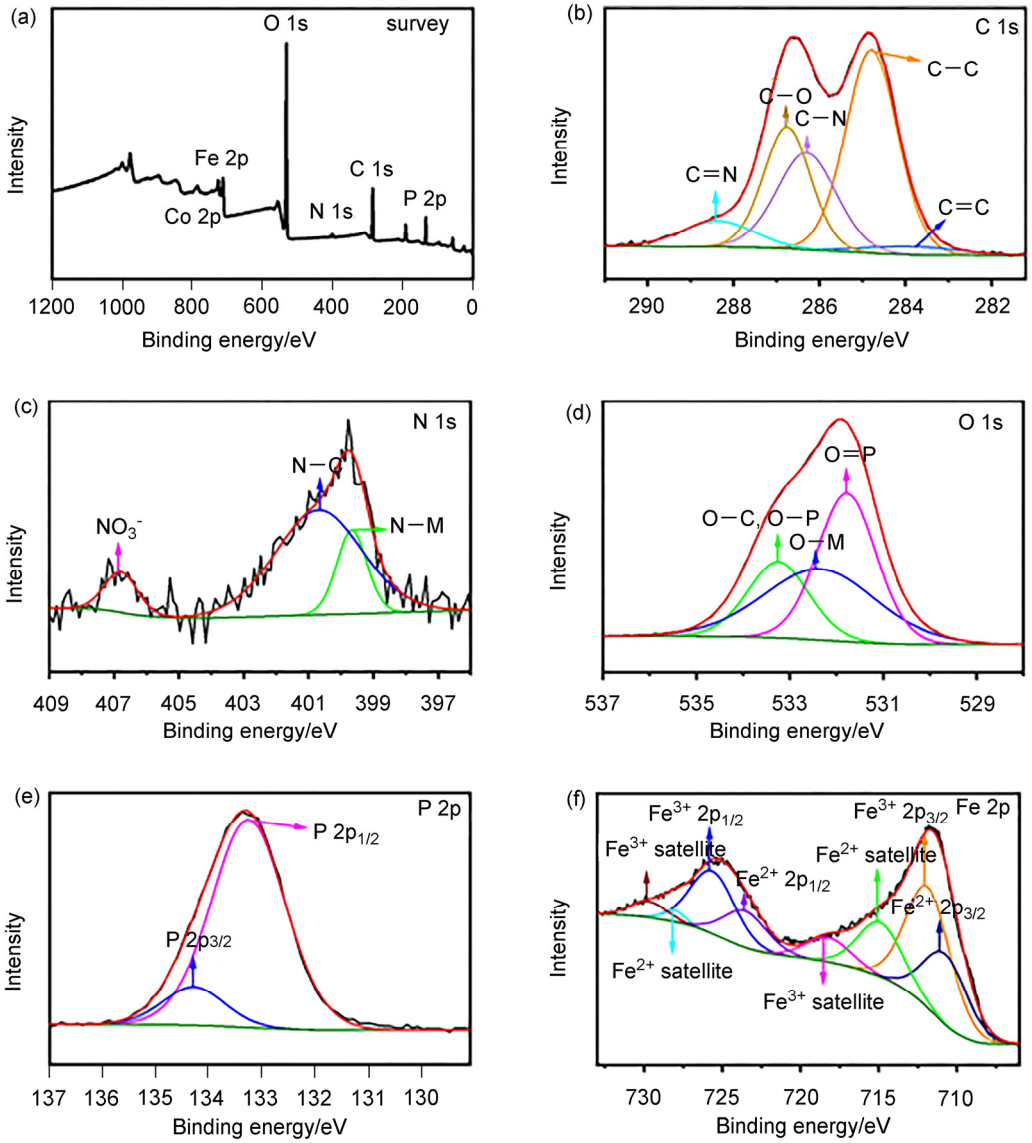

Figure 2 (a) XPS spectrum of ZIF-L-Co@PA-Fe, and high-resolution spectra of (b) C 1s, (c) N 1s, (d) O 1s, (e) P 2p, and (f) Fe 2p

2.2 Catalytic performance

Iron complexes have already been extensively applied to construct C—N, C—O, and C—S bonds through a hydrogen transfer strategy.[22] Using this iron based metal-organic hybrid, the synthesis of benzoxazoles via acceptorless dehydrogenative coupling of alcohols with 2-nitrophenol was explored. The model reaction of 2-nitrophenol (**1a**) and benzyl alcohol (**2a**) was conducted to evaluate the catalytic performance of the catalysts. Obviously, the reaction cannot take place without catalysts, while upon the addition of ZIF-L-Co@PA-Fe, cyclization reaction proceeded with the expected product being noticed (Table 1, Entries 1, 2). Formation of the product 2-phenylbenzoxazole (**3aa**) was not observed when the reaction was carried out in the presence of $Fe(NO_3)_3$ or ZIF-L-Co as catalysts at solvent-free conditions (Entries 3, 4). The introduction of PA could increase the yield of benzoxazole to 35%, possibly because PA destroyed ZIF-L-Co and in the meanwhile released a portion of the metal active site of Co (Entry 5). When different amounts of Fe^{3+} were exchanged with ZIF-L-Co@PA, the catalytic performance of ZIF-L-Co@PA-Fe-*x* was greatly changed (Entries 6～9). When the concentration of Fe^{3+} used for cation exchange was less than 0.04 mol•L^{-1}, the resulting catalysts still showed low catalytic activity (<35%). As the increase of Fe^{3+} exchanged, the catalytic activity of ZIF-L-Co@PA-Fe-*x* increased at first and then remain unchanged. ZIF-L-Co@PA-Fe-0.08 exhibited the highest yield of 80% (Entry 2). Fe confined in the metal-organic hybrids was critical for the high catalytic activity. In contrast, PA-Fe synthesized by directly precipitation was also used for the reaction under similar reaction conditions, but no desired product was detected (Entry 10). ZIF-L-Co@PA-Fe prepared via ligand-cation successive exchange inherited the structural

 © 2023 Shanghai Institute of Organic Chemistry, Chinese Academy of Sciences

Table 1 Optimization of reaction conditions[a]

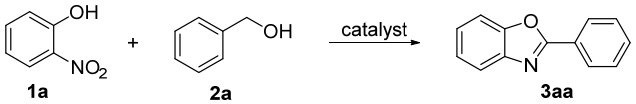

Entry	Catalyst	Base	Solvent	Temp./℃	Yield[b]/%
1	—	—	—	150	＜5
2	ZIF-L-Co@PA-Fe-0.08	—	—	150	80
3	$Fe(NO_3)_3$	—	—	150	5
4	ZIF-L-Co			150	5
5	PA	—	—	150	35
6	ZIF-L-Co@PA-Fe-0.02	—	—	150	10
7	ZIF-L-Co@PA-Fe-0.04	—	—	150	35
8	ZIF-L-Co@PA-Fe-0.06	—	—	150	61
9	ZIF-L-Co@PA-Fe-0.1	—	—	150	78
10	PA-Fe	—	—	150	＜5
11	ZIF-L-Co@PA-Fe-0.08	—	DMF	150	＜5
12	ZIF-L-Co@PA-Fe-0.08	—	DMSO	150	＜5
13	ZIF-L-Co@PA-Fe-0.08	—	Toluene	150	33
14	ZIF-L-Co@PA-Fe-0.08	—	*p*-Xylene	150	68
15	ZIF-L-Co@PA-Fe-0.08	KO^{t}Bu	—	150	44
16	ZIF-L-Co@PA-Fe-0.08	KOH	—	150	19
17	ZIF-L-Co@PA-Fe-0.08	NaO^{t}Bu	—	150	37
18	ZIF-L-Co@PA-Fe-0.08	Cs_2CO_3	—	150	51
19	ZIF-L-Co@PA-Fe-0.08	K_2CO_3	—	150	42
20	ZIF-L-Co@PA-Fe-0.08	—	—	130	55
21	ZIF-L-Co@PA-Fe-0.08	—	—	110	43
22[c]	**ZIF-L-Co@PA-Fe-0.08**	—	—	**150**	**86**
23[d]	ZIF-L-Co@PA-Fe-0.08	—	—	150	46

[a] Reagents and conditions: **1a** (1 mmol), **2a** (3 mmol), base (0.5 equiv.), catalyst (20 mg), solvent (2 mL), 24 h, air. [b] Yields of isolated product. [c] N_2. [d] O_2.

characteristics of ZIF-L-Co and showed significantly enhanced catalytic activity in this reaction. Therefore, catalytic activity depends on both of the composition and structure of ZIF-L-Co@PA-Fe. Solvents such as *N*,*N*-dimethylformamide (DMF), dimethylsulfoxide (DMSO), toluene and *p*-xylene were evaluated for this reaction. The reaction gave the maximum yield of the product under solvent-free conditions (Entries 2 and 11～14). Bases as co-catalysts were also studied but furnished the targeted product in lower yields than base-free conditions (Entries 15～19). The reaction temperature was another important factor. The yields of products decreased as temperature fell (Entries 2 and 20, 21). Moreover, O_2 was proved to be unfavorable condition for this reaction, but N_2 was suitable for the reaction with a much higher yield of **3aa** (Table 1, Entries 2 and 22, 23).

With the optimized condition in hand (Table 1, Entry 22), the general applicability of ZIF-L-Co@PA-Fe catalyst was tested for the synthesis of substituted benzoxazoles using various derivatives of 2-nitrophenols (**1**) and benzyl alcohols (**2**), and the results are summarized in Table 2. A series of functional groups including methyl-, methoxy-, chloro-, bromo-, and fluoro-substituted benzyl alcohols (**2**) were all well tolerated under the optimal reaction conditions with high yileds of desired products over 80% (Table 2, **3aa**～**3aq**). The yields of benzyl alcohol containing electron-withdrawing groups were slightly higher than electron-donating groups, especially 4-trifluoromethyl benzyl alcohol, which could obtain product at 90% yield (Table 2, **3ad**). Generally, alcohols with *para*-substituents provided the desired products in slightly higher yields than the corresponding *meta*- and *ortho*-substituents (Table 2, **3ab**～**3ar**). It was worth noting that 3,5-bis(trifluoromethyl)benzyl alcohol realized a yield of 91% (Table 2, **3as**). Alcohols bearing nitrogen heterocycle groups (2-pyridine, 3-pyridine based) also acquired the desired products with 76% and 70% yields respectively (Table 2, **3as** and **3at**). In order to extend the reaction scope, various substituted *o*-nitrophenols were also employed to react with **2** under the optimized conditions. 2-Nitrophenol containing electron donating substituents (such as methyl and methoxy) and electron withdrawing substituents (such as chloro, bromo, and fluoro) all could react smoothly with benzyl alcohol and provide yields more than 70% (Table 2, **3ba**～**3fa**). The electron withdrawing substituents have slightly higher yields than the electron donating ones. The position of the substituents on the phenyl ring of 2-nitrophenol has little effect on the reaction yield (Table 2, **3da** and **3ga**).

2.3 Mechanistic investigations

Control experiments were performed to investigate the reaction mechanism. No products were detected when the

 © 2023 Shanghai Institute of Organic Chemistry, Chinese Academy of Sciences

Table 2 Substrates expansion of 2-phenylbenzoxazoles[a,b]

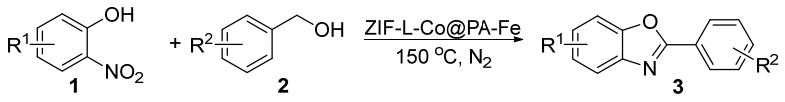

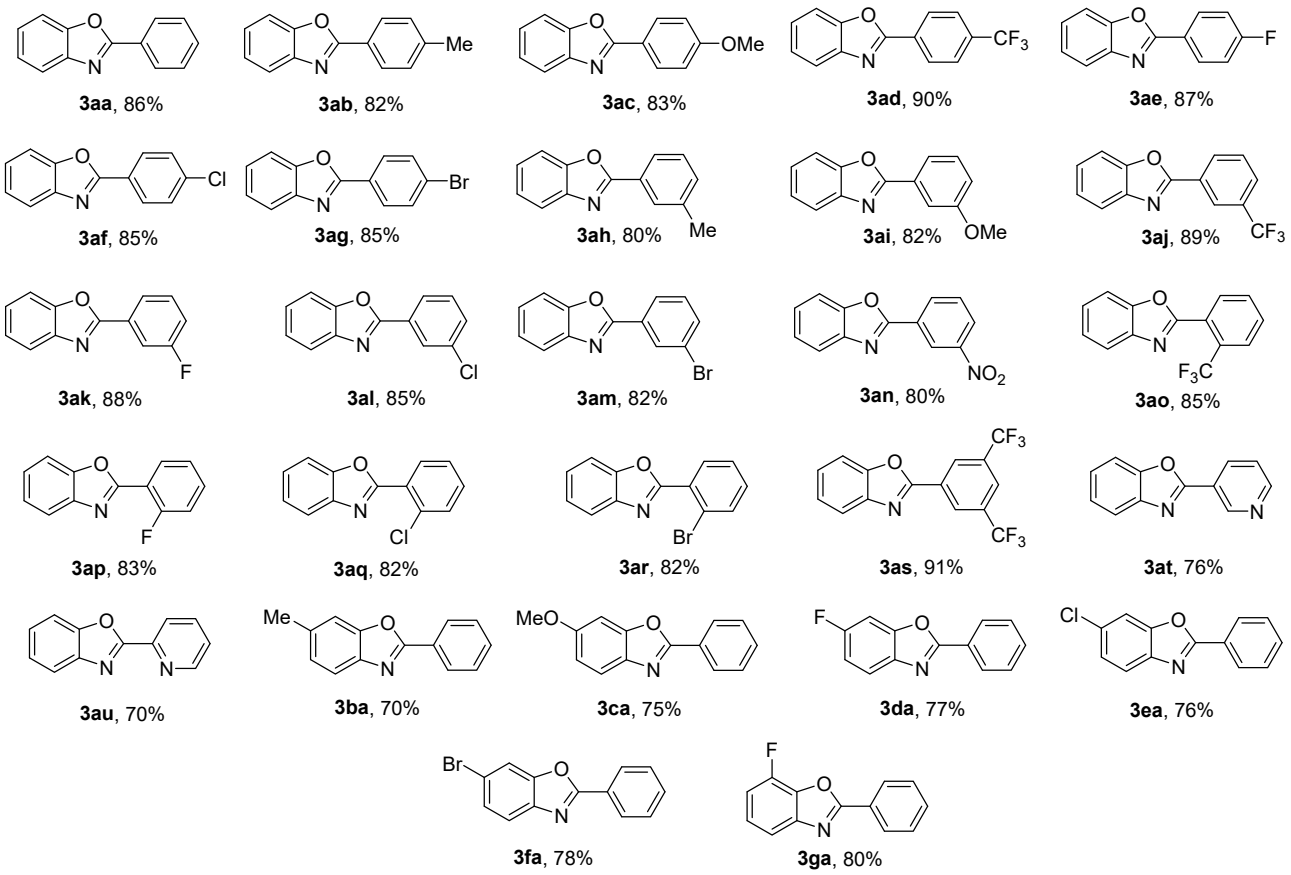

[a] Reagents and conditions: the reaction was carried out with **1** (1.0 mmol), **2** (3.0 mmol) and ZIF-L-Co@PA-Fe (20 mg) under N_2 at 150 ℃ for 24 h. [b] Yields of isolated product.

reaction was carried out without ZIF-L-Co@PA-Fe, indicating ZIF-L-Co@PA-Fe catalyst played an important role in this hydrogen transfer reaction (Scheme 2, a). As shown in Scheme 2b, benzaldehyde was applied to react with 2-nitrophenol instead of benzyl alcohol. However, nitro reduction of *o*-nitrophenol did not occur and no products were observed. While *o*-aminophenol was treated with benzyl alcohol, no desired product was detected as well (Scheme 2, c). It was speculated that benzyl alcohol as hydrogen donor and 2-nitrophenol as hydrogen acceptor were indispensable for iron-phytate complex catalyzed hydrogen transfer reactions for benzoxazole formation (Scheme 2, b and c).

A plausible mechanism illustrated in Scheme 3 for the synthesis of benzoxazole catalyzed by ZIF-L-Co@PA-Fe was proposed based on the above-described experiments. ZIF-L-Co@PA-Fe coordination complex mediates the oxidation of alcohol and reduction of nitrophenol as hydrogen carriers. The oxidation of benzyl alcohol results in reduced metal (Fe^{2+}/Co^{2+}) species, which stimulate the reduction step of *o*-nitro phenol to aminophenol. Condensation of the oxidized aldehyde with reduced aminophenolgenerates imine intermediates. A second hydrogen-transfer process from imine via cyclization and oxidation with oxidized metal species (Fe^{3+}/Co^{3+}) provides the

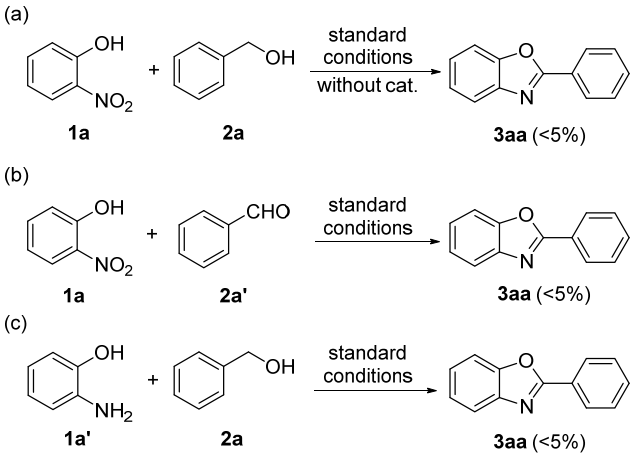

Scheme 2 Control experiments

 © 2023 Shanghai Institute of Organic Chemistry, Chinese Academy of Sciences

desired product benzoxazole. The reversible metal center of prepared complex is crucial to the accomplishment of dehydrogenation-hydrogenation process.

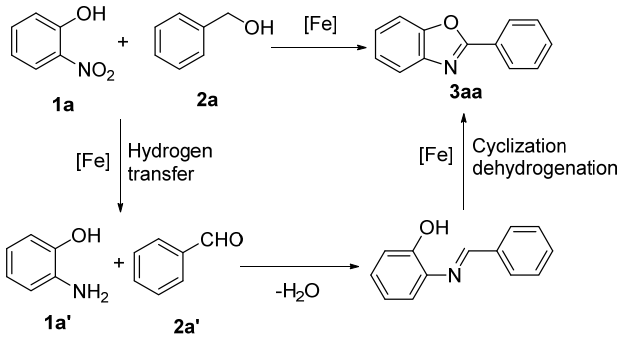

Scheme 3 Proposed mechanism for the synthesis of benzoxazole

Based on the above mechanism, we conducted several sets of intermediates capture experiments since the capture of intermediates often plays a crucial role in the mechanism exploration. Benzyl alcohol could transform into benzaldehyde in a low yield under standard conditions (Scheme 4, a). Further experiment disclosed that intermediate imine was successfully cyclized and dehydrogenated to produce the target product with the assistant of 2-nitrophenol under standard conditions, which indicated that the proposed mechanism was possible.

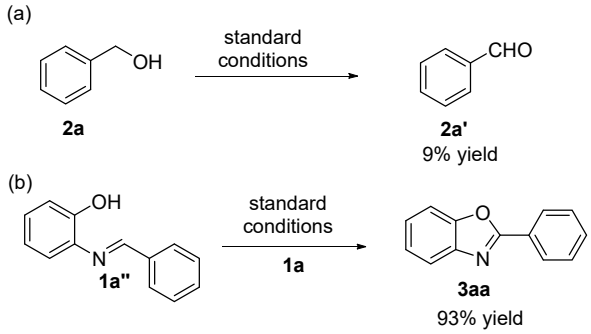

Scheme 4 Mechanism verification

2.4 Reusability of the catalyst

The stability and reusability of ZIF-L-Co@PA-Fe was also evaluated in this work. Circulation experiments were performed under standard conditions for benzoxazole synthesis. It was found that ZIF-L-Co@PA-Fe could be reused for at least five cycles without appreciably reducing the yield of benzoxazole (Scheme 5). The recovered ZIF-L-Co@PA-Fe was further characterized by SEM and fourier transform infrared spectroscopy (FT-IR), which indicated that the properties of ZIF-L-Co@PA-Fe were not changed notably after being reused.

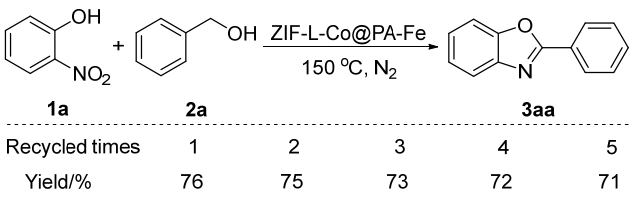

Recycled times	1	2	3	4	5
Yield/%	76	75	73	72	71

Scheme 5 Recycled experiments

3 Conclusions

In conclusion, an inexpensive iron catalyst was designed for catalytic synthesis of a variety of benzoxazoles under solvent-free conditions, utilizing hydrogen transfer reaction from alcohols. ZIF-L-Co@PA-Fe metal-organic hybrid was fabricated by exchange reactions from metal organic frameworks. The incorporation of phytic acid and Fe^{3+} enabled ZIF-L-Co to achieve remarkable catalytic flexibility in the synthesis of benzoxazoles. ZIF-L-Co@PA-Fe hybrids applied for benzoxazoles formation via a hydrogen transfer strategy between nitro and alcohol functionalities showed yields up to 90%. The enhanced catalytic performance of ZIF-L-Co@PA-Fe was attribute to the reversible metal center, nanosheet morphology and hetero-structures. As a heterogeneous catalyst, ZIF-L-Co@PA-Fe not only exhibited outstanding catalytic activity but also showed excellent stability. This work provides a general approach for fabricating metal-organic hybrid catalysts via a MOF-templated post-synthetic pathway.

4 Experimental section

4.1 General methods and materials

All commercial reagents and solvents were obtained from the commercial provider and used without further purification. All the obtained products were characterized by ^{1}H NMR, ^{13}C NMR and referenced to DMSO-d_6 (δ 2.50 for ^{1}H NMR, and δ 39.5 for ^{13}C NMR) or $CDCl_3$ (δ 7.26 for ^{1}H NMR, and δ 77.1 for ^{13}C NMR) with tetramethylsilane as internal standard (δ 0). ^{1}H NMR and ^{13}C NMR spectra were obtained on a Varian 400 or 101 MHz respectively on a Bruker Advance III HD 400 MHz spectrometer. Analytical thin layer chromatography (TLC) was performed using commercially prepared 100～400 mesh silica gel plates (SGF254). Flash column chromatography was performed on 230～430 mesh silica gel. SEM image was performed on a HITACHI S-4800 field-emission scanning electron microscope. XPS data were recorded with electron energy analyzer (ESCALAB 250Xi, Thermo Fisher Co, USA). IR spectra were recorded on total reflection Fourier infrared spectrometer (NICOLET 6700). X-ray diffraction (XRD) was recorded on a Bruker D8 Advance X-ray diffractometer.

4.2 Preparation of ZIF-L-Co, ZIF-L-Co@PA, ZIF-L-Co@PA-Fe and PA-Fe complex

4.2.1 Representative procedure for the synthesis of ZIF-L-Co

In a typical synthesis, aqueous solutions of 2-methylimidazole (2-MIM, 0.4 mmol/mL) and $Co(NO_3)_2$ (0.4 mmol/mL) were prepared, respectively. Then, 5 mL of

 © 2023 Shanghai Institute of Organic Chemistry, Chinese Academy of Sciences

prepared $Co(NO_3)_2$ was added to 40 mL of 2-MIM solution and kept stirring for 2 h at room temperature. ZIF-L-Co was obtained after centrifugation and washed several times with deionized water and methanol until the supernatant became colorless.

4.2.2 Representative procedure for the synthesis of phytic acid treated ZIF-L-Co.

Typically, the prepared ZIF-L-Co above was re-dispersed in methanol (70 mL) upon ultrasonication. Thereafter, an aqueous solution of phytic acid (140 mL, 1.25 mg/mL) was quickly added into the ZIF-L-Co dispersion. The mixture was then allowed to keep stirring for 1 h. Finally, the acid-treated products were separated by centrifugation, washed with ethanol, and vacuum dried overnight at 60 ℃.

4.2.3 Representative procedure for the synthesis of ZIF-L-Co@PA-Fe.

Typically, 150 mg of the obtained ZIF-L-Co@PA was re-dispersed in deionized water (1 mg/mL). Then an aqueous solution of iron nitrate (75 mL, 0.02, 0.04, 0.06, 0.08, 0.10 mol/L) was added. The resulting mixture reacted under stirring at room temperature for 3 h. Product was obtained by centrifugation and washed several times with deionized water and ethanol. Finally, the samples were vacuum dried overnight at 60 ℃ and denoted as ZIF-L-Co@PA-Fe-0.02, ZIF-L-Co@PA-Fe-0.04, ZIF-L-Co@PA-Fe-0.06, ZIF-L-Co@PA-Fe-0.08, ZIF-L-Co@PA-Fe-0.1.

4.2.4 Representative procedure for the synthesis of PA-Fe complex.

Typically, 0.06 mol of Fe $(NO_3)_3$•$9H_2O$ was dissolved in 100 mL of EtOH. Then 50 mL of phytic acid ethanol solution (0.2 mol/L) was added dropwise. The mixture was kept stirring at 80 ℃ for 2 h. The PA-Fe complex was obtained by centrifugation and washed several times with deionized water and ethanol.

4.3 General procedure for the synthesis of benzoxazoles

ZIF-L-Co@PA-Fe-0.08 (20 mg), nitrophenol (1.0 mmol, 1 equiv.) and alcohol (3.0 mmol, 3 equiv.) were sealed in a 25 mL tube. The catalytic reaction was carried out under a nitrogen atmosphere at 150 ℃ for 24 h. After termination of the reactions, the mixture was concentrated under vacuum to give a crude product. The crude product was purified by column chromatography, and eluted with petroleum ether/ethyl acetate to afford the desired products.

2-Phenylbenzo[*d*]oxazole (**3aa**): White solid (167.7 mg, 86%). m.p. 102～105 ℃ (Lit.[8] 103～105 ℃); ^{1}H NMR (400 MHz, $CDCl_3$) δ: 8.29～8.23 (m, 2H), 7.81～7.75 (m, 1H), 7.60～7.56 (m, 1H), 7.53 (dd, J=5.2, 2.0 Hz, 3H), 7.35 (dd, J=6.0, 3.2 Hz, 2H); ^{13}C NMR (101 MHz, $CDCl_3$) δ: 163.16, 150.85, 142.18, 131.66, 129.04, 127.73, 127.24, 125.24, 124.71, 120.12, 110.72.

2-(*p*-Tolyl)benzo[*d*]oxazole (**3ab**): White solid (171.4 mg, 82%). m.p. 115～117 ℃ (Lit.[8] 115～117 ℃); ^{1}H NMR (400 MHz, $CDCl_3$) δ: 8.13 (d, J=8.2 Hz, 2H), 7.78～7.73 (m, 1H), 7.58～7.52 (m, 1H), 7.35～7.28 (m, 4H), 2.42 (s, 3H); ^{13}C NMR (101 MHz, $CDCl_3$) δ: 163.31, 150.70, 142.20, 142.07, 129.66, 127.61, 124.88, 124.50, 124.42, 119.86, 110.51, 21.66.

2-(4-Methoxyphenyl)benzo[*d*]oxazole (**3ac**): White solid (186.7 mg, 83%). m.p. 102～105 ℃ (Lit.[8] 102～104 ℃); ^{1}H NMR (400 MHz, $CDCl_3$) δ: 8.09 (d, J=8.5 Hz, 2H), 7.68～7.60 (m, 1H), 7.44 (dd, J=6.5, 2.6 Hz, 1H), 7.18～7.25 (m, J=5.6 Hz, 2H), 6.91 (d, J=8.7 Hz, 2H), 3.77 (s, 3H); ^{13}C NMR (101 MHz, $CDCl_3$) δ: 162.13, 161.29, 149.65, 141.26, 128.34, 123.54, 123.36, 118.67, 118.58, 113.31, 109.33, 54.38.

2-(4-(Trifluoromethyl)phenyl)benzo[*d*]oxazole (**3ad**): White solid (236.7 mg, 90%). m.p. 139～142 ℃ (Lit.[8] 142～144 ℃); ^{1}H NMR (400 MHz, $CDCl_3$) δ: 8.34 (dp, J=7.7, 0.8 Hz, 2H), 7.80～7.73 (m, 3H), 7.60～7.55 (m, 1H), 7.41～7.34 (m, 2H); ^{13}C NMR (101 MHz, $CDCl_3$) δ: 161.55, 150.93, 141.97, 133.05 (q, J=32.7 Hz), 130.49, 127.93, 126.01 (q, J=3.7 Hz), 125.91, 125.03, 123.85 (q, J=271.7 Hz), 120.48, 110.89.

2-(4-Fluorophenyl)benzo[*d*]oxazole (**3ae**): White solid (185.3 mg, 87%). m.p. 98～101 ℃ (Lit.[8] 97～99 ℃); ^{1}H NMR (400 MHz, $CDCl_3$) δ: 8.24 (ddd, J=9.0, 5.3, 0.9 Hz, 2H), 7.78～7.72 (m, 1H), 7.55 (ddt, J=6.4, 3.7, 0.8 Hz, 1H), 7.34 (ddd, J=6.4, 3.2, 0.7 Hz, 2H), 7.19 (ddd, J=9.1, 8.4, 0.9 Hz, 2H); ^{13}C NMR (101 MHz, $CDCl_3$) δ: 164.91 (d, J=252.0 Hz), 162.26, 150.85, 142.12, 129.93 (d, J=9.0 Hz), 125.25, 124.77, 123.56 (d, J=4.0 Hz), 120.07, 116.29 (d, J=22.0 Hz), 110.67.

2-(4-Chlorophenyl)benzo[*d*]oxazole (**3af**): White solid (195.1 mg, 85%). m.p. 151～155 ℃ (Lit.[8] 150～152 ℃); ^{1}H NMR (400 MHz, $CDCl_3$) δ: 8.20～8.15 (m, 2H), 7.78～7.72 (m, 1H), 7.59～7.54 (m, 1H), 7.49 (d, J=2.0 Hz, 1H), 7.49～7.47 (m, 1H), 7.38～7.33 (m, 2H); ^{13}C NMR (101 MHz, $CDCl_3$) δ: 162.17, 150.84, 142.07, 137.87, 129.39, 128.95, 125.73, 125.47, 124.86, 120.18, 110.74.

2-(4-Bromophenyl)benzo[*d*]oxazole (**3ag**): White solid (232.9 mg, 85%). m.p. 157～160 ℃ (Lit.[8] 156～158 ℃); ^{1}H NMR (400 MHz, $CDCl_3$) δ: 8.13～8.06 (m, 2H), 7.78～7.73 (m, 1H), 7.67～7.62 (m, 2H), 7.58～7.54 (m, 1H), 7.38～7.32 (m, 2H); ^{13}C NMR (101 MHz, $CDCl_3$) δ: 162.24, 150.83, 142.08, 132.34, 129.10, 126.34, 126.17, 125.50, 124.87, 120.20, 110.75.

2-(*m*-Tolyl)benzo[*d*]oxazole (**3ah**): White solid (167.2 mg, 80%). m.p. 81～83 ℃ (Lit.[8] 81～83 ℃); ^{1}H NMR (400 MHz, $CDCl_3$) δ: 8.10～8.00 (m, 2H), 7.80～7.74 (m, 1H), 7.58～7.53 (m, 1H), 7.40～7.30 (m, 4H), 2.43 (s, 3H); ^{13}C NMR (101 MHz, $CDCl_3$) δ: 163.34, 150.83, 142.21, 138.81, 132.46, 128.92, 128.29, 127.10, 125.13, 124.86, 124.64, 120.05, 110.65, 21.44.

2-(3-Methoxyphenyl)benzo[*d*]oxazole (**3ai**): White solid (184.5 mg, 82%). m.p. 73～76 ℃ (Lit.[23a] 72～74 ℃); ^{1}H NMR (400 MHz, $CDCl_3$)) δ: 7.88～7.81 (m, 1H), 7.77 (ddd, J=6.5, 3.8, 2.3 Hz, 2H), 7.61～7.52 (m, 1H), 7.41 (t, J=8.0 Hz, 1H), 7.34 (dq, J=6.2, 3.6 Hz, 2H), 7.11～7.01 (m, 1H), 3.90 (s, 3H); ^{13}C NMR (101 MHz, $CDCl_3$)) δ:

 © 2023 Shanghai Institute of Organic Chemistry, Chinese Academy of Sciences

163.06, 160.03, 150.83, 142.12, 130.11, 128.41, 125.28, 124.71, 120.21, 120.10, 118.45, 111.95, 110.72, 55.61.

2-(3-(Trifluoromethyl)phenyl)benzo[*d*]oxazole (**3aj**): White solid (234.1 mg, 89%). m.p. 119～121 ℃ (Lit.[23a] 119～122 ℃); ^{1}H NMR (400 MHz, $CDCl_3$) δ: 8.53 (s, 1H), 8.43 (d, J=7.8 Hz, 1H), 7.82～7.75 (m, 2H), 7.68～7.58 (m, 2H), 7.42～7.35 (m, 2H); ^{13}C NMR (101 MHz, $CDCl_3$) δ: 161.49, 150.81, 141.86, 131.62 (q, J=32.7 Hz), 130.61, 129.55, 128.04, 127.93 (q, J=3.7 Hz) ,125.73, 124.94, 124.51 (q, J=4.0 Hz), 123.72 (q, J=271.0 Hz), 120.32, 110.78.

2-(3-Fluorophenyl)benzo[*d*]oxazole (**3ak**): White solid (187.4 mg, 88%). m.p. 91～95 ℃ (Lit.[23a] 92～94 ℃); ^{1}H NMR (400 MHz, $CDCl_3$) δ: 8.02 (ddd, J=7.8, 1.6, 1.0 Hz, 1H), 7.92 (ddd, J=9.4, 2.7, 1.6 Hz, 1H), 7.79～7.74 (m, 1H), 7.59～7.54 (m, 1H), 7.47 (td, J=8.1, 5.7 Hz, 1H), 7.38～7.32 (m, 2H), 7.21 (tdd, J=8.3, 2.6, 1.0 Hz, 1H); ^{13}C NMR (101 MHz, $CDCl_3$) δ: 163.00 (d, J=246.3 Hz), 161.88 (d, J=3.8 Hz), 150.84, 142.00, 130.73 (q, J=8.0 Hz), 129.26 (d, J=8.6 Hz), 125.61, 124.89, 123.40 (d, J=2.9 Hz), 120.31, 118.60 (d, J=21.0 Hz), 114.63 (d, J=24.0 Hz), 110.79.

2-(3-Chlorophenyl)benzo[*d*]oxazole (**3al**): White solid (195.8 mg, 85%). m.p. 120～124 ℃ (Lit.[23a] 122～124 ℃); ^{1}H NMR (400 MHz, $CDCl_3$) δ: 8.23 (t, J=1.7 Hz, 1H), 8.11 (dt, J=7.5, 1.5 Hz, 1H), 7.79～7.73 (m, 1H), 7.59～7.54 (m, 1H), 7.50～7.41 (m, 2H), 7.38～7.33 (m, 2H); ^{13}C NMR (101 MHz, $CDCl_3$) δ: 161.72, 150.85, 141.97, 135.15, 131.59, 130.33, 128.91, 127.69, 125.72, 125.65, 124.92, 120.31, 110.81.

2-(3-Bromophenyl)benzo[*d*]oxazole (**3am**): White solid (224.68 mg, 82%). m.p. 128～130 ℃ (Lit.[23a] 128～130 ℃); ^{1}H NMR (400 MHz, $CDCl_3$) δ: 8.40 (t, J=1.8 Hz, 1H), 8.16 (ddd, J=7.8, 1.6, 1.0 Hz, 1H), 7.79～7.74 (m, 1H), 7.63 (ddd, J=8.0, 2.0, 1.1 Hz, 1H), 7.59～7.55 (m, 1H), 7.40～7.33 (m, 3H); ^{13}C NMR (101 MHz, $CDCl_3$) δ: 161.46, 150.77, 141.90, 134.39, 130.49, 130.45, 129.05, 126.07, 125.56, 124.83, 123.02, 120.23, 110.71.

2-(3-Nitrophenyl)benzo[*d*]oxazole (**3an**): White solid (192 mg, 80%). m.p. 205～211 ℃ (Lit.[23b] 210～214 ℃); ^{1}H NMR (400 MHz, $CDCl_3$) δ: 9.07 (t, J=2.0 Hz, 1H), 8.57 (ddd, J=7.8, 1.7, 1.1 Hz, 1H), 8.37 (ddd, J=8.2, 2.3, 1.1 Hz, 1H), 7.82～7.77 (m, 1H), 7.72 (t, J=8.0 Hz, 1H), 7.64～7.60 (m, 1H), 7.44～7.38 (m, 2H); ^{13}C NMR (101 MHz, $CDCl_3$) δ: 160.66, 150.96, 148.78, 141.86, 133.13, 130.24, 129.02, 126.19, 125.90, 125.23, 122.58, 120.60, 111.00.

2-(2-(Trifluoromethyl)phenyl)benzo[*d*]oxazole (**3ao**): White solid (223.5 mg, 85%). m.p. 67～70 ℃; ^{1}H NMR (400 MHz, $CDCl_3$) δ: 8.13 (ddd, J=7.2, 1.6, 0.8 Hz, 1H), 7.90～7.80 (m, 2H), 7.71～7.58 (m, 3H), 7.43～7.35 (m, 2H); ^{13}C NMR (101 MHz, $CDCl_3$) δ: 161.26, 151.31, 141.70, 132.30, 132.02, 131.14, 129.26 (q, J=32.3 Hz), 127.18 (q, J=5.3 Hz), 126.25, 125.77, 124.85, 123.55 (q, J=272.0 Hz), 120.64, 111.01.

2-(2-Fluorophenyl)benzo[*d*]oxazole (**3ap**): White solid (176.8 mg, 83%). m.p. 96～99 ℃ (Lit.[8] 97～99 ℃); ^{1}H NMR (400 MHz, $CDCl_3$) δ: 8.22 (td, J=7.5, 1.8 Hz, 1H), 7.89～7.78 (m, 1H), 7.63～7.57 (m, 1H), 7.53～7.47 (m, 1H), 7.39～7.33 (m, 2H), 7.31～7.22 (m, 2H); ^{13}C NMR (101 MHz, $CDCl_3$) δ: 162.20, 159.62, 150.55, 141.86, 133.23 (d, J=8.7 Hz), 130.62, 125.60, 124.80, 124.61 (d, J=3.9 Hz), 120.47, 117.20 (d, J=22.1 Hz), 115.60 (d, J=8.9 Hz), 110.81.

2-(2-Chlorophenyl)benzo[*d*]oxazole (**3aq**): White solid (188.2 mg, 82%). m.p. 71～74 ℃ (Lit.[23a] 72～74 ℃); ^{1}H NMR (400 MHz, $CDCl_3$) δ: 8.16～8.11 (m, 1H), 7.87～7.81 (m, 1H), 7.63～7.58 (m, 1H), 7.57～7.52 (m, 1H), 7.46～7.35 (m, 4H); ^{13}C NMR (101 MHz, $CDCl_3$) δ: 161.05, 150.66, 141.78, 133.56, 132.00, 131.92, 131.50, 127.03, 126.32, 125.67, 124.78, 120.61, 110.85.

2-(2-Bromophenyl)benzo[*d*]oxazole (**3ar**): yellow solid (224.7 mg, 82%). m.p. 54～56 ℃ (Lit.[23c] 54～56 ℃); ^{1}H NMR (400 MHz, $CDCl_3$) δ: 8.07 (dd, J=7.8, 1.8 Hz, 1H), 7.87～7.82 (m, 1H), 7.76 (dd, J=8.0, 1.2 Hz, 1H), 7.64～7.58 (m, 1H), 7.45 (td, J=7.6, 1.2 Hz, 1H), 7.41～7.32 (m, 3H); ^{13}C NMR (101 MHz, $CDCl_3$) δ: 161.64, 150.74, 141.72, 134.79, 132.26, 132.12, 128.47, 127.57, 125.69, 124.77, 122.01, 120.64, 110.89.

2-(3,5-bis(Trifluoromethyl)phenyl)benzo[*d*]oxazole (**3as**): White solid (301.2 mg, 91%). m.p. 168～170 ℃ (Lit.[23d] 168～170 ℃); ^{1}H NMR (400 MHz, $CDCl_3$) δ: 8.64 (dt, J=1.9, 0.8 Hz, 2H), 7.99 (dq, J=1.7, 0.8 Hz, 1H), 7.76 (ddd, J=6.6, 1.7, 0.7 Hz, 1H), 7.60～7.55 (m, 1H), 7.42～7.34 (m, 2H); ^{13}C NMR (101 MHz, $CDCl_3$) δ: 159.95, 150.88, 141.66, 132.70 (q, J=33.7 Hz), 129.31, 127.47, 126.38, 125.35, 124.64 (q, J=3.7 Hz), 123.00 (q, J=272.7 Hz), 120.67, 110.97.

2-(Pyridin-3-yl)benzo[*d*]oxazole (**3at**): White solid (149.0 mg, 76%). m.p. 112～114 ℃ (Lit.[8] 112～114 ℃); ^{1}H NMR (400 MHz, $CDCl_3$) δ: 8.78 (ddd, J=4.8, 1.8, 1.0 Hz, 1H), 8.32 (dt, J=8.0, 1.1 Hz, 1H), 7.88～7.77 (m, 2H), 7.66～7.60 (m, 1H), 7.43～7.34 (m, 3H); ^{13}C NMR (101 MHz, $CDCl_3$) δ: 161.52, 151.12, 150.37, 146.11, 141.83, 137.19, 126.14, 125.67, 125.03, 123.53, 120.71, 111.32.

2-(Pyridin-2-yl)benzo[*d*]oxazole (**3au**): yellow solid (137.2 mg, 70%). m.p. 111～114 ℃; ^{1}H NMR (400 MHz, $CDCl_3$) δ: 9.47 (s, 1H), 8.76 (s, 1H), 8.50 (d, J=8.2 Hz, 1H), 7.85～7.74 (m, 1H), 7.64～7.57 (m, 1H), 7.50～7.34 (m, 3H); ^{13}C NMR (101 MHz, $CDCl_3$) δ: 160.81, 152.12, 150.85, 148.83, 141.86, 134.84, 125.85, 125.04, 123.84, 120.39, 110.89.

6-Methyl-2-phenylbenzo[*d*]oxazole (**3ba**): White solid (146.3 mg, 70%). m.p. 91～93 ℃ (Lit.[8] 93～95 ℃); ^{1}H NMR (400 MHz, $CDCl_3$) δ: 8.27～8.20 (m, 2H), 7.63 (d, J=8.2 Hz, 1H), 7.53～7.48 (m, 3H), 7.37 (dt, J=1.5, 0.7 Hz, 1H), 7.16 (ddd, J=8.1, 1.6, 0.7 Hz, 1H), 2.49 (s, 3H); ^{13}C NMR (101 MHz, $CDCl_3$) δ: 161.45, 149.96, 138.84, 134.46, 130.18, 127.77, 126.37, 126.27, 124.72, 118.25, 109.68, 20.72.

6-Methoxy-2-phenylbenzo[*d*]oxazole (**3ca**): White solid (168.7 mg, 75%). m.p. 71～73 ℃ (Lit.[23b] 90～72 ℃); ^{1}H NMR (400 MHz, $CDCl_3$) δ: 8.16～8.08 (m, 2H), 7.56

 © 2023 Shanghai Institute of Organic Chemistry, Chinese Academy of Sciences

(d, J=8.7 Hz, 1H), 7.43 (q, J=2.8 Hz, 3H), 7.03 (d, J=2.4 Hz, 1H), 6.88 (dd, J=8.7, 2.4 Hz, 1H), 3.80 (s, 3H). ^{13}C NMR (101 MHz, $CDCl_3$) δ: 161.22, 157.27, 150.63, 134.86, 130.04, 127.84, 126.34, 126.17, 118.96, 111.80, 94.42, 54.92.

6-Fluoro-2-phenylbenzo[*d*]oxazole (**3da**): White solid (164.0 mg, 77%). m.p. 105～107 ℃ (Lit.[8] 109～111 ℃); ^{1}H NMR (400 MHz, $CDCl_3$) δ: 8.23～8.15 (m, 2H), 7.67 (dd, J=8.7, 4.9 Hz, 1H), 7.50 (qd, J=4.8, 1.6 Hz, 3H), 7.28 (dd, J=8.0, 2.4 Hz, 1H), 7.08 (td, J=9.2, 2.4 Hz, 1H); ^{13}C NMR (101 MHz, $CDCl_3$) δ: 163.68 (d, J=3.1 Hz), 160.67 (d, J=242.5 Hz), 150.70 (d, J=15.0 Hz), 138.42 (q, J=1.9 Hz), 131.59, 128.95, 127.48, 126.87, 120.25 (q, J=9.8 Hz), 112.54 (q, J=25.7 Hz), 98.67 (q, J=14.0 Hz).

6-Chloro-2-phenylbenzo[*d*]oxazole (**3ea**): White solid (174.4 mg, 76%). m.p. 104～107 ℃ (Lit.[23e] 104～106 ℃); ^{1}H NMR (400 MHz, $CDCl_3$) δ: 8.15 (dd, J=7.7, 2.0 Hz, 2H), 7.60 (d, J=8.5 Hz, 1H), 7.52 (d, J=1.9 Hz, 1H), 7.48～7.42 (m, 3H), 7.26 (dd, J=8.5, 2.0 Hz, 1H); ^{13}C NMR (101 MHz, $CDCl_3$) δ: 163.74, 150.95, 140.92, 131.84, 130.70, 129.00, 127.69, 126.74, 125.32, 120.49, 111.27.

6-Bromo-2-phenylbenzo[*d*]oxazole (**3fa**): White solid (213.7 mg, 78%). m.p. 89～91 ℃ (Lit.[23f] 89～91 ℃); ^{1}H NMR (400 MHz, $CDCl_3$) δ: 8.11 (dd, J=7.7, 1.8 Hz, 2H), 7.62 (d, J=1.8 Hz, 1H), 7.51 (d, J=8.5 Hz, 1H), 7.45～7.39 (m, 3H), 7.36 (dd, J=8.4, 1.8 Hz, 1H); ^{13}C NMR (101 MHz, $CDCl_3$) δ: 162.46, 150.13, 140.25, 130.77, 127.91, 126.95, 126.63, 125.59, 119.87, 116.91, 113.05.

7-Fluoro-2-phenylbenzo[*d*]oxazole (**3ga**): White solid (170.4 mg, 80%). m.p. 97～102 ℃; ^{1}H NMR (400 MHz, $CDCl_3$) δ: 8.23～8.15 (m, 2H), 7.50～7.41 (m, 4H), 7.22～7.17 (m, 1H), 7.05～6.98 (m, 1H); ^{13}C NMR (101 MHz, $CDCl_3$) δ: 162.53, 146.04 (d, J=252.0 Hz), 144.31 (d, J=2.0 Hz), 136.80 (d, J=10.7 Hz), 130.91, 127.95, 126.83, 125.49, 123.91 (d, J=5.9 Hz), 114.75 (d, J=4.1 Hz), 110.83 (d, J=16.3 Hz).

Supporting Information Characterizations of ZIF-L-Co@PA-Fe and NMR spectra of compounds **3aa**～**3ga**. The Supporting Information is available free of charge via the Internet at http://sioc-journal.cn.

References

[1] (a) Demmer, C. S.; Bunch, L. *Eur. J. Med. Chem.* **2015**, *97*, 778.
(b) Jiang, B.; Shi, S. *Chin. J. Org. Chem.* **2022**, *42*, 3263 (in Chinese).
(蒋滨阳, 施世良, 有机化学, **2022**, *42*, 3263.)
(c) Horton, D. A.; Bourne, G. T.; Smythe, M. L. *Chem. Rev.* **2003**, *103*, 893.
(d) Li, J.; Liu, H.; Zhang, B.; Ge, B.; Wang, D. *Chin. J. Org. Chem.* **2022**, *42*, 619 (in Chinese).
(李家豪, 刘洪强, 张博, 葛冰洋, 王大伟, 有机化学, **2022**, *42*, 619.)
(e) Asensio, J. A.; Sánchez, E. M.; Gomez-Romero, P. *Chem. Soc. Rev.* **2010**, *39*, 3210.
(f) Zhao, J.; Jin, Z.; Wang, R.; Zhang, X.; Han, Y.; Hu, C.; Liu, X.; Zhang, C.; Jin, L. *Chin. J. Org. Chem.* **2022**, *42*, 2172 (in Chinese).
(赵静, 金辄, 王润, 张新庚, 韩英妹, 胡春, 刘晓平, 张传明, 金丽萍, 有机化学, **2022**, *42*, 2172.)
(g) Shi, Y. M.; Crames, J. J.; Czech, L.; Bozhüyük, K. A. J.; Shi, Y. N.; Hirschmann, M.; Lamberth, S.; Claus, P.; Paczia, N.; Rückert, C.; Kalinowski, J.; Bange, G.; Bode, H. B. *Angew. Chem., Int. Ed.* **2022**, *134*, e202206106.
(h) Tan, Z.; Jiang, H.; Zhang, M. *Chem. Commun.* **2016**, *52*, 9359.
(i) Yadav, G.; Ganguly, S. *Eur. J. Med. Chem.* **2015**, *97*, 419.
(j) Hikawa, H.; Ichinose, R.; Kikkawa, S.; Azumaya, I. *Green Chem.* **2018**, *20*, 1297.

[2] (a) Saranya, T. V.; Sruthi, P. R.; Raj, V.; Anas, S. *J. Organomet. Chem.* **2021**, *937*, 121733.
(b) Mishra, N.; Singh, A. S.; Agrahari, A. K.; Singh, S. K.; Singh, M.; Tiwari, V. K. *ACS Comb. Sci.* **2019**, *21*, 389.
(c) Urzúa, J. I.; Contreras, R.; Salas, C. O.; Tapia, R. A. *RSC Adv.* **2016**, *6*, 82401.
(d) Zhao, M.; Yang, Z.; Yang, D. *Chin. J. Org. Chem.* **2022**, *42*, 111 (in Chinese).
(赵咪娜, 杨梓墨, 杨得锁, 有机化学, **2022**, *42*, 111.)
(e) Hajipour, A. R.; Khorsandi, Z. A. *New J. Chem.* **2016**, *40*, 10474.
(f) Hao, S.; Yang, J.; Liu, P.; Xu, J., Yang, C.; Li, F. *Org. Lett.* **2021**, *23*, 2553.
(g) Hu, X.; Yang, B.; Yao, W.; Wang, D. *Chin. J. Org. Chem.* **2018**, *38*, 3296 (in Chinese).
(胡昕宇, 杨伯斌, 姚玮, 王大伟, 有机化学, **2018**, *38*, 3296.)
(h) Saha, P.; Ramana, T.; Purkait, N.; Ashif, M. A.; Pau, R.; Punniyamurth, T. *J. Org. Chem.* **2009**, *74*, 8719.
(i) Tang, Y.; Li, M.; Gao, H.; Rao, G.; Mao, Z. *RSC Adv.* **2020**, *10*, 14317.

[3] (a) Moghaddam, F. M.; Saberi, V.; Kalhor, S.; Veisi, N. *Appl. Organomet. Chem.* **2018**, *32*, e4240.
(b) Sahu, P. K. *RSC Adv.* **2017**, *7*, 42000.
(c) Li, Z.; Wang, Q.; Pu, M.; Yang, Z.; Lei, M. *Acta Chim. Sinica* **2020**, *78*, 437 (in Chinese).
(李哲伟, 王骞阅, 蒲敏, 杨作银, 雷鸣, 化学学报, **2020**, *78*, 437.)
(d) Bahrami, K.; Bakhtiarian, M. *ChemistrySelect* **2018**, *3*, 10875.
(e) Liu, P.; Tung, N. T.; Xu, X.; Yang, J.; Feng, L. *J. Org. Chem.* **2021**, *86*, 2621.
(f) Shebitha, A. M.; Shaibuna, M.; Hiba, K.; Sreekuma, K. *Catal. Lett.* **2022**, *152*, 3017.
(g) Inamdar, S. M.; More, V. K.; Mandal, S. K. *Tetrahedron Lett.* **2013**, *54*, 579.
(h) Hikawa, H.; Nakayama, T.; Takahashi, M.; Kikkawa, S.; Azumaya, I. *Adv. Synth. Catal.* **2021**, *363*, 4075.
(i) Ma, C.; Huang, Y.; Zhao, Y. *ACS Catal.* **2016**, *6*, 6408.

[4] (a) Ferlin, F.; van der Hulst, M. K.; Santoro, S.; Lanari, D.; Vaccaro, L. *Green Chem.* **2019**, *21*, 5298.
(b) Chen, R.; Jalili, Z.; Tayebee, R. *RSC Adv.* **2021**, *11*, 16359.
(c) Safaei, E.; Alaji, Z.; Panahi, F.; Wojtczak, A.; Jagličić, J. Z. *New J. Chem.* **2018**, *42*, 7230.
(d) Hu, J.; Li, M.; Wan, J.; Sun, J.; Gao, H.; Zhang, F.; Zhang, Z. *Org. Biomol. Chem.* **2022**, *20*, 3413.
(e) Khalafi-Nezhad, A.; Panahi, F. *ACS Catal.* **2014**, *4*, 1686.
(f) Jiang, H.; Zang, C.; Cheng, H.; Sun, B.; Gao, X. *Catal. Sci. Technol.* **2021**, *11*, 7955.
(g) Doan, S. H.; Tran, C. B.; Cao, An, L. N.; Le, N. T. H.; Phan, N. T. S. *Catal. Lett.* **2019**, *149*, 2053.
(h) Feng, X.; Xu, C.; Wang, Z.; Tang, S.; Fu, W.; Ji, B.; Wang, L. *Inorg. Chem.* **2015**, *54*, 2088.
(i) Yu, J.; Shen, M.; Lu, M. *J. Iran. Chem. Soc.* **2015**, *12*, 771.
(j) Prakash, G.; Ramachandran, R.; Nirmala, M.; Viswanathamurthi, P.; Linert, W. *Monatsh. Chem.* **2014**, *145*, 1903.
(k) Narang, U.; Yadav, K. K.; Bhattacharya, S.; Chauhan, S. M. S. *ChemistrySelect* **2017**, *2*, 7135.

 © 2023 Shanghai Institute of Organic Chemistry, Chinese Academy of Sciences

(l) Li, J.; Liu, H.; Zhu, H.; Yao, W.; Wang, D. *ChemCatChem* **2021**, *13*, 4751.
(m) Yu, J.; Xu, J.; Lu, M. *Appl. Organomet. Chem.* **2013**, *27*, 606.
(n) Endo, Y.; Bäckvall, J. E. *Chem.-Eur. J.* **2012**, *18*, 13609.
(o) Li, J.; Yang, Y.; Hu, W.; Xia, X.; Wang, D. *Chin. J. Org. Chem.* **2022**, *42*, 190 (in Chinese).
(李家豪, 杨义科, 胡文康, 夏晓峰, 王大伟, 有机化学, **2022**, *42*, 190.)
(p) Yu, H.; Wada, K.; Fukutake, T.; Feng, Q.; Uemura, S.; Isoda, K.; Hirai, T.; Iwamoto, S. *Catal. Today* **2021**, *375*, 410.
(q) Ramachandran, R.; Prakash, G.; Selvamurugan, S.; Viswanathamurthi, P.; Malecki, J. G.; Ramkumar, V. *Dalton Trans.* **2014**, *43*, 7889.
(r) Lai, Y. L.; Ye, J. S.; Huang, J. M. *Chem.-Eur. J.* **2016**, *22*, 5425.

[5] (a) Cao, F.; Duan, Z.; Zhu, H.; Wang, D. *Mol. Catal.* **2021**, *503*, 111391.
(b) Khalili, D.; Banazadeh, A. R. *Bull. Chem. Soc. Jpn.* **2015**, *88*, 1693.
(c) Bains, A. K.; Dey, D.; Yadav, S.; Kundu, A.; Adhikari, D. *Catal. Sci. Technol.* **2020**, *10*, 6495.
(d) Liu, X.; Kuang, C.; Su, C. *Acta Chim. Sinica* **2022**, *80*, 1135 (in Chinese).
(刘霞, 匡春香, 苏长会, 化学学报, **2022**, *80*, 1135.)
(e) Chakraborty, G.; Mondal, R.; Guin, A. K.; Paul, N. D. *Org. Biomol. Chem.* **2021**, *19*, 7217.
(f) Kaldhi, D.; Vodnala, N.; Gujjarappa, R.; Nayak, S.; Ravichandiran, V.; Gupta, S.; Hazra, C. K.; Malakar, C. C. *Tetrahedron Lett.* **2019**, *60*, 223.
(g) Li, J.; Mao, A.; Yao, W.; Zhu, H.; Wang, D. *Green Chem.* **2022**, *24*, 2602.
(h) Samanta, P. K.; Ray, S.; Das, T.; Gage, S. H.; Nandi, M.; Richards, R. M.; Biswas, P. *Microporous Mesoporous Mater.* **2019**, *284*, 186.
(i) Guang, R.; Zhao, H.; Zhang, M. *Org. Lett.* **2022**, *24*, 3048.
(j) Wilfred, C. D.; Taylor, R. J. K. *Synlett* **2004**, 1628.
(k) Mohanty, A.; Roy, S. *Tetrahedron Lett.* **2016**, *57*, 2749.
(l) Liu, J.; Wang, C.; Ma, X.; Shi, X.; Wang, X.; Li, H.; Xu, Q. *Catal. Lett.* **2016**, *146*, 2139.
(m) Xu, Z.; Yu, X.; Sang, X.; Wang, D. *Green Chem.* **2018**, *20*, 2571.

[6] (a) Das, K.; Waiba, S.; Jana, A.; Maji, B. *Chem. Soc. Rev.* **2022**, *51*, 4396.
(b) Borthakur, I.; Sau, A.; Kundu, S. *Coordin. Chem. Rev.* **2022**, *451*, 214257.
(c) Irrgang, T.; Kempe, R. *Chem. Rev.* **2019**, *119*, 2524.
(d) Wei, D.; Darcel, C. *Chem. Rev.* **2019**, *119*, 2550.
(e) Hey, D. A.; Reich, R. M.; Baratta, W.; Kühn, F. E. *Chem. Rev.* **2018**, *374*, 114.
(f) Corma, A.; Navas, J.; Sabater, M J. *Chem. Rev.* **2018**, *119* 1410.
(g) Goyal, V.; Sarki, N.; Narani, A.; Naik, G.; Natte, K.; Jagadeesh, R. V. *Coord. Chem. Rev.* **2023**, *474*, 214827.
(h) Podyacheva, E.; Afanasyev, O. I.; Vasilyev, D. V.; Chusov, D. *ACS Catal.* **2022**, *12*, 7142.
(i) Tong, T.; Douthwaite, M.; Chen, L.; Engel, R.; Conway, M. B.; Guo, W.; Wu, X.; Gong, X.; Wang, Y.; Morgan, D. J.; Davies, T.; Kiely, C. J.; Chen, L.; Liu, X.; Hutchings, G. J. *ACS Catal.* **2023**, *13*, 1207.
(j) Wang, S.; Song, D.; Shen, F.; Chen, R.; Cheng, Y.; Zhao, C.; Shen, Q.; Yin, S.; Ling, F.; Zhong, W. *Green Chem.* **2023**, *25*, 357.
(k) Jin, M. Y.; Zhou, Y.; Xiao, D.; You, Y.; Zhen, Q.; Tao, G.; Yu, P.; Xing, X. *Angew. Chem., Int. Ed.* **2022**, *61*, e202112993.

[7] Wu, M.; Hu, X.; Liu, J.; Liao, Y.; Deng, G. *Org. Lett.* **2012**, *14*, 2722.

[8] Putta, R. R.; Chun, S.; Choi, S. H.; Lee, S. H.; Oh, D.; Hong, S. *J. Org. Chem.* **2020**, *85*, 15396.

[9] Tang, L.; Guo, X.; Yang, Y.; Zha, Z.; Wang, Z. *Chem. Commun.* **2014**, *50*, 6145.

[10] (a) Sen, C.; Sahoo, T.; Galani, S. M.; Panda, A. B.; Ghosh, S. C. *ChemistrySelect* **2016**, *1*, 2542.
(b) Chaurasia, S. R.; Bhanage, B. M. *ChemistrySelect* **2018**, *3*, 7963.

[11] (a) Banerjee, R.; Phan, A.; Wang, B.; Knobler, C.; Furukawa, H.; O'Keeffe, M.; Yaghi, O. M. *Science* **2008**, *319*, 939.
(b) Banerjee, R.; Furukawa, H.; Britt, D.; Knobler, C.; O'Keeffe, M.; Yaghi, O. M. *J. Am. Chem. Soc.* **2009**, *131*, 3875.
(c) Chen, R.; Yao, J.; Gu, Q.; Smeets, S.; Baerlocher, C.; Gu, H.; Zhu, D.; Morris, W.; Yaghi, O. M.; Wang, H. *Chem. Commun.* **2013**, *49*, 95002.
(d) Jia, H.; Xie, R.; Lu, G.; Jiang, H.; Zhang, M. *ACS Catal.* **2022**, *12*, 10294.
(e) Feng, Y.; Wang, H.; Yao, J. *Coord. Chem. Rev.* **2021**, *431*, 213677.

[12] (a) Zanon, A.; Verpoort, F. *Coord. Chem. Rev.* **2017**, *353*, 201.
(b) Cheng, N.; Ren, L.; Xu, X.; Du, Y.; Dou, S. X. *Adv. Energy Mater.* **2018**, *8*, 1801257.
(c) Duan, C.; Yu, Y.; Hu, H. *Green Energy Environ.* **2020**, *29*, 827.

[13] (a) Ma, D.; Li, B.; Shi, Z. *Chin. Chem. Lett.* **2018**, *29*, 827.
(b) Qin, Y.; Li, Z.; Duan, Y.; Guo, J.; Zhao, M.; Tang, Z. *Matter* **2022**, *5*, 3260.
(c) Wang, Y.; Chen, L.; Hou, C. C.; Wei, Y. S.; Xu, Q. *Org. Biomol. Chem.* **2020**, *18*, 8508.

[14] (a) Park, H.; Oh, S.; Lee, S.; Choi, S.; Oh, M. *Appl. Catal., B* **2019**, *246*, 322.
(b) Zhang, C.; Yang, H.; Zhong, D.; Xu, Y.; Wang, Y.; Yuan, Q.; Liang, Z.; Wang, B.; Zhang, W.; Zheng, H.; Cheng, T.; Cao, R. *J. Mater. Chem. A* **2020**, *8*, 9536.
(c) Guo, F.; He, Y.; Zeng, H.; Liu, H.; Yang, D.; Chen, H.; Li, H.; Liu, Y. *Colloids Surf., A* **2022**, *648*, 129417.

[15] Zhang, J.; Zhang, T.; Yu, D.; Xiao, K.; Hong, Y. *CrystEngComm* **2015**, *17*, 8212.

[16] Chen, M.; Peng, C.; Su, Y.; Chen, X.; Zhang, Y.; Wang, Y.; Peng, J. *Angew. Chem., Int. Ed.* **2020**, *59*, 20988.

[17] Fu, H.; Wang, Z.; Wang, X.; Wang, P.; Wang, C. C. *CrystEngComm* **2018**, *20*, 1473.

[18] (a) Hao, Y.; Sani, L A.; Ge, T.; Fang, Q. *Appl. Surf. Sci.* **2017**, *419*, 826.
(b) Sun. X.; Xu, W.; Zhang, X.; Lei, T.; Lee, S. Y.; Wu, Q. *J. Energy Chem.* **2021**, *52*, 170.
(c) Ong, J. Y.; Ng, X. Q.; Lu, S.; Zhao, Y. *Org. Lett.* **2020**, *22*, 6447.
(d) He, J.; Jiao, L.; Cheng, X.; Chen, G.; Wu, Q.; Wang, X.; Yang, L.; Hu, Z. *Acta Chim. Sinica* **2022**, *80*, 896 (in Chinese).
(何家伟, 焦柳, 程雪怡, 陈光海, 吴强, 王喜章, 杨立军, 胡征, 化学学报, **2022**, *80*, 896.)

[19] (a) Sasikumar, B.; Arthanareeswaran, G. *Appl. Surf. Sci.* **2022**, *606*, 154900.
(b) Wang, D.; Hu, J.; Li, Y.; Fu, M.; Liu, D.; Chen, Q. *J. Membr. Sci*. **2016**, *501*, 228.

[20] (a) Zárate-Guzmán, A. I.; González-Gutiérrez, L. V.; Ocampo-Pérez, R.; Carrasco-Marín, F.; Romero-Cano, L. A. *J. Water Process Eng.* **2020**, *36*, 101273.
(b) Gao, X.; Cao, Z.; Li, C.; Liu, J.; Liu, X.; Guo, L. *New J. Chem.* **2022**, *46*, 18952.

[21] Liu, H.; Wei, G.; Xu, Z.; Liu, P.; Li, Y. *Appl. Surf. Sci.* **2016**, *389*, 438.

[22] (a) Quintard, A.; Rodriguez, J. *Angew. Chem. Int. Ed.* **2014**, *53*, 4044.
(b) Yan, T.; Feringa, B. L.; Barta, K. *Nat. Commun.* **2014**, *5*, 5602.
(c) Quintard, A.; Constantieux, T.; Rodriguez, J. *Angew. Chem., Int. Ed.* **2013**, *52*, 12883.
(d) Pan, H. J.; Lin, Y.; Gao, T.; Lau, K. K.; Feng, W.; Yang, B.; Zhao, Y. *Angew. Chem., Int. Ed.* **2021**, *133*, 18747.
(e) Elangovan, S.; Sortais, J. B.; Beller, M.; Darcel, C. *Angew. Chem., Int. Ed.* **2015**, *54*, 14483.
(f) Polidano, K.; Allen, B. D. W.; Williams, J. M. J.; Morrill, L. C. *ACS Catal.* **2018**, *8*, 6440.
(g) Bettoni, L.; Gaillard, S.; Renaud, J. L. *Org. Lett.* **2020**, *22*,

 © 2023 Shanghai Institute of Organic Chemistry, Chinese Academy of Sciences

2064.
(h) Chang, S.; Liu, H.; Shi, G.; Xia, X.; Wang, D.; Duan, Z. *New J. Chem.* **2022**, *46*, 15929.
(i) Bettoni, L.; Gaillard, S.; Renaud, J. L. *Org. Lett.* **2019**, *21*, 8404.
(j) Guo, N.; Zhu, S. *Chin. J. Org. Chem.* **2015**, *35*, 1383 (in Chinese).
(郭娜, 朱守非, 有机化学, **2015**, *35*, 1383.)
[23] (a) Singh, A. S.; Singh, M.; Mishra, N.; Mishra, S.; Agrahari, A. K.; Tiwari, V. K. *ChemistrySelect* **2017**, *2*, 154.
(b) Mishra, N.; Singh, A. S.; Agrahari, A. K.; Singh, S. K.; Singh, M.; Tiwari, V. K. *ACS Appl. Energy Mater.* **2019**, *21*, 389.
(c) Patra, A.; James, A.; Das, T. K.; Biju, A. T. *J. Org. Chem.* **2018**, *83*, 14820.
(d) Meeniga, I.; Gokanapalli, A.; Peddiahgari, V. G. R. *Sustainable Chem. Pharm.* **2022**, *30*, 100874.
(e) Boissarie, P. J.; Hamilton, Z. E.; Lang, S.; Murphy, J. A.; Suckling, C. J. *Org. Lett.* **2011**, *13*, 6256.
(f) Leng, Y.; Yang, F.; Zhu, W.; Zou, D.; Wu, Y.; Cai, R. *Tetrahedron* **2011**, *67*, 6191.

(Zhao, C.)

 © 2023 Shanghai Institute of Organic Chemistry, Chinese Academy of Sciences